Experimental observation of stimulated low-frequency Raman scattering in water suspensions of silver and gold nanoparticles

N. V. Tcherniega,[1] K. I. Zemskov,[1] V. V. Savranskii,[2] A. D. Kudryavtseva,[1,*] A. Y. Olenin,[3] and G. V. Lisichkin[3]

[1]*P. N. Lebedev Physical Institute, Russian Academy of Sciences, Leninskii pr. 53, Moscow 119991, Russia*

[2]*A. M. Prokhorov General Physics Institute, Russian Academy of Sciences, Vavilov Str. 38, Moscow 119991, Russia*

[3]*Chemistry Department, M. V. Lomonosov Moscow State University, Vorob'evy Gory, Moscow 119991, Russia*

**Corresponding author: akudr@sci.lebedev.ru*

Received December 20, 2012; revised February 7, 2013; accepted February 7, 2013;
posted February 8, 2013 (Doc. ID 182142); published March 5, 2013

In this Letter we report on experimental observation of stimulated low-frequency Raman scattering (SLFRS) in gold and silver nanoparticle suspensions excited by 20 ns ruby laser pulses, SLFRS propagated in forward and backward directions with a maximum conversion efficiency up to 20%. Frequency shift for silver nanoparticle suspension was found to be 0.33 THz and for gold nanoparticle suspension 0.435 THz. This type of stimulated scattering of light can be used as an effective source of biharmonic pumping for solving a large number of practical tasks. © 2013 Optical Society of America

OCIS codes: 290.5890, 160.4236.

Theoretical and experimental investigation of the peculiarities of inelastic light scattering caused by acoustic vibration of nanoparticles has attracted great attention since the first experimental observation of the sized-quantized acoustic modes in microcrystals with the help of low-frequency Raman scattering (LFRS) [1]. The acoustical properties of an elastic sphere with stress-free boundary conditions were studied by Lamb [2]. It was shown that two types of acoustic modes (spheroidal and torsional), labeled by the angular momentum number l and by the quantum number n, exist. Only the Raman active modes can be seen in the LFRS spectrum. In the case of an elastic sphere, spheroidal symmetric $l = 0$ and quadrupolar $l = 2$ spheroidal modes are Raman active [3]. The investigation of the small particle vibrational mode structure becomes more complicated if effects of the particle coupling to the surrounding matrix or damping of the modes due to acoustical radiation from the nanoparticle into the surrounding medium are taken into consideration [4,5]. LFRS in semiconductor, dielectric, and metallic nano-objects [6–8] gives important information about their vibrational dynamics.

The size dependence of the vibrational properties of nanosized particles is important for a basic understanding of their properties and determination of their potential optoelectronic applications. The frequency shift of the scattered light is defined by the eigenfrequencies of the particles. Spontaneous LFRS is typically a very weak process with nearly spatially isotropic emission. It is known that for every type of spontaneous scattering of light caused by fluctuations of the optical properties, the stimulated scattering of light exists [9]. In the case of stimulated scattering, the fluctuations are induced by an initial light field, and this fact defines the high efficiency and spatial properties of the scattered light (direction of propagation, divergence). At some conditions of excitation the stimulated low-frequency Raman scattering (SLFRS) of light can be excited. Stimulated scattering of light by the acoustic vibrations of monodisperse silica spheres in synthetic opal matrices was realized with high conversion efficiency [10]. A high-efficiency inelastic scattering of light due to optoacoustic interaction in nanostructured thin films of different types was registered [11]. Active materials used in these works can be considered as quasi-homogeneous media with the acoustic and optical properties totally defined by the acoustic and optical properties of the individual units of submicron size. In this Letter we report on the experimental observation of SLFRS with high-conversion efficiency in suspensions of gold and silver nanoparticles. Low-frequency confined acoustic phonons in silver and gold nanoparticles define the SLFRS first Stokes component frequency shift.

Preliminarily synthesized gold and silver nanoparticle aqueous suspensions were used as active media. Preparative methods for silver and gold nanoparticle suspensions were analogous and only quantities of used reagents were different. All synthesis was carried out in 100 ml chemical glass in the ultrasonic field generated by ultrasonic bath PSB 2835-05. Before synthesis distilled water was poured into the glass, then CTAB and metal precursor were inserted in this liquid medium, and the mixture was irradiated for 10 min for micellar medium formation. Afterward, 5 ml freshly prepared solution of sodium borohydrate was injected for 10 min. Then the mixture was kept under ultrasonic irradiation for 20 min. Metal precursors and quantities of reagents are presented in Table 1.

Prepared silver aqueous suspension was used as an adsorbent with no extra chemical pretreatment upon 10-fold dilution with distilled water (diluted aqueous sol). The absorption spectrum of the silver aqueous suspension was monitored to stay unchanged for at least 2 weeks after its synthesis. The analogous method was used for gold nanoparticle preparation [12].

Electron microphotographs and histograms of size distribution for gold and silver nanoparticle suspension are presented in Fig. 1.

Ruby laser giant pulses ($\lambda = 694.3$ nm, $\tau = 20$ ns, $E_{\max} = 0.3$ J, $\Delta\nu = 0.015$ cm^{-1}) were used as the source

Table 1. Metal Precursors and Quantities of Reagents used at Metal Suspension Preparation

Metal	V ml[a]	Q1[b]	M[c]	Q2[d]	Q3[e]
Ag	20.00	0.44 g (1.2 mmol)	$AgNO_3$	0.17 g (1 mmol)	0.72 g (2 mmol)
Au	19.78	0.044 g (0.12 mmol)	$HAuCl_4$	0.22 mL 0.44M solution (0.1 mmol)	0.072 g (0.2 mmol)

[a]Volume of initial distilled water, ml.
[b]Quantity of initial distilled water.
[c]Metal precursor.
[d]Quantity of metal precursor.
[e]Quantity of sodium borohydrate.

of excitation. The exciting light was focused into the material by lenses with different focal lengths (50, 90, and 150 mm). The length of the cell with suspension was 3 cm. The sample distance from the focusing system and exciting light energy were also changed, which allowed us to vary the power density at the entrance of the sample and field distribution inside the sample. Investigations were conducted for the different energy and geometrical conditions of excitation.

Fabry–Perot interferometers were used for laser light passing through the cell and scattered light in the backward direction spectral structure investigations. The range of dispersion was changed from 0.42 to 16.7 cm^{-1}. All measurements were realized for both forward and backward directions (for the light passing through the sample and for the light reflected from the sample). A mirror was used to register the initial light spectrum simultaneously with the spectrum of the scattered light in the backward direction.

Under ruby laser pulse excitation we observed in all samples investigated the first Stokes component of SLFRS of light in the case of laser intensity exceeding the threshold value. SLFRS was observed in backward (opposite to the initial pumping beam) and forward directions. At the experimental conditions of excitation only the first Stokes component was excited. Figure 2 shows the typical interferogram for the first Stokes component excited in Ag suspension propagating in the backward direction. Figure 2(a) corresponds to laser pulse intensity 0.075 GW/cm^2. Only one system of rings that corresponds to the laser pulse is registered by Fabry–Perot interferometer. When the laser pulse intensity exceeds the threshold value (for Ag suspension $P = 0.09$ GW/cm^2), an additional system of rings that corresponds to the SLFRS appeared [see Fig. 2(b)].

Frequency shift of the scattered light was the same for forward and backward SLFRS for each sample. Maximum energy conversion of the laser light into the SLFRS light was in the range of 0.1–0.2 and was defined by the geometrical and energetical conditions of excitation. The divergence of the light scattered in the backward direction was of the order of 10^{-3} rad. The linewidth of the scattered light was of the order of the laser light linewidth. It is necessary to mention that at the experimental conditions of excitation in the cell filled with water stimulated Brillouin scattering (SBS), propagating in the backward direction was registered (see Table 2). In Ag and Au suspensions SBS was not registered. This fact is connected with the impossibility of the effective hypersound wave formation due to spatial inhomogeneities of suspensions.

The frequency of confined acoustic phonons defines the frequency shift of the first Stokes component, which is proportional to sound velocity in the material and inversely proportional to the size of the nanoparticles. The vibrational motion of a homogeneous elastic sphere with

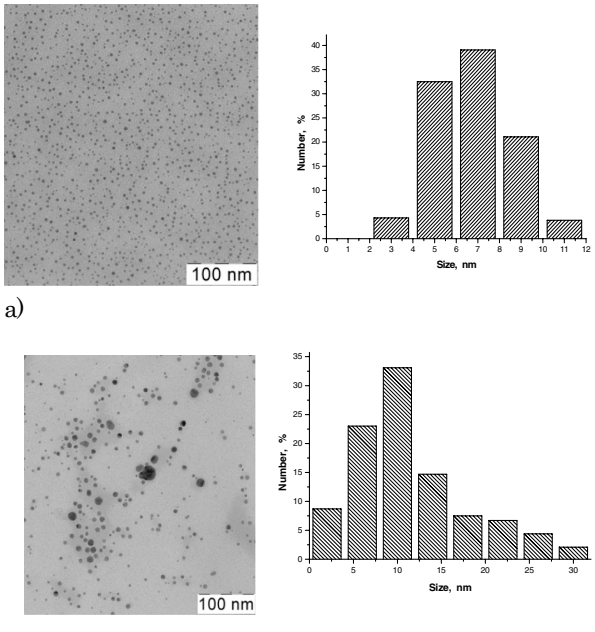

Fig. 1. Electron microphotography and histogram of size distribution for (a) suspension of gold nanoparticles and (b) suspension of silver nanoparticles.

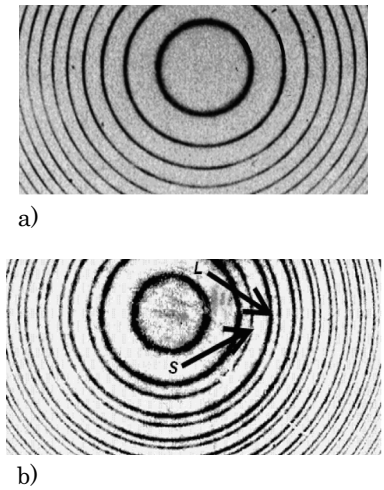

Fig. 2. Interferogram of (a) laser pulse, (b) laser (L) and SLFRS (S) pulses.

Table 2. SLFRS and SBS Characteristics

Sample	η^a%	P^b GW/cm^2	$\Delta\nu^c$ THz	D^d nm	$D_1{}^e$ nm
Ag suspension	20	0.09	0.33	9.9	9.89
Au suspension	12	0.1	0.435	7.1	6.95
H_2O (SBS)	10	0.07	0.0058	—	—

[a]SLFRS maximum conversion efficiency.
[b]Threshold.
[c]Shift of the first Stokes component frequency.
[d]Theoretical value of the nanoparticle diameter that corresponds to the lowest order spheroidal mode.
[e]Nanoparticle diameter value corresponding to the histogram of the size distribution maximum for Ag and Au suspensions.

free surface has been theoretically studied [2,4]. Lowest order spheroidal radial and quadrupolar modes are Raman active and can be observed in spontaneous Raman spectra. Our measured values of the scattered light spectral peak positions of 0.33 and 0.435 THz for Ag and Au suspensions, respectively, correspond to the lowest order spheroidal modes for Ag and Au spheres with diameter 9.9 and 7.1 nm. These values are very close to the nanoparticle diameter values that correspond to the maximum nanoparticle concentration (see Table 1). In our experimental conditions of excitation more intense modes (spheroidal radial mode) are being amplified from the noise level and define the SLFRS spectral properties. SLFRS is caused by the nonlinear interaction between the nanoparticle vibrations with frequency $\Delta\nu$ and the optical field. Induced polarization of the metal nanoparticles that is modulated by a nanoparticle vibration is the source of the spontaneous LFRS. LFRS is typically a very weak process with efficiency about 10^{-6} with nearly isotropic emission. In the case of the SLFRS, which is a third-order nonlinear optical process, the nanoparticle vibrations are excited by two optical fields—the laser and the LFRS. These two fields are driving the interaction with the nanoparticles and can lead to strong SLFRS amplification. At the experimental conditions for Ag suspension 20% of the energy of the laser pulse was converted into the SLFRS pulse energy. The SLFRS process leads to emission in a narrow cone in the backward and forward directions. The divergence of the SLFRS beams propagating in forward and backward directions was about 10^{-3} rad.

SLFRS demonstrates very narrow linewidth that is of the order of the laser linewidth at the experimental conditions of excitation. A spectral narrowing of the stimulated scattering of light compared to the spontaneous scattering band usually occurs at high excitation intensities.

It is interesting to compare the parameters of SLFRS with the parameters of SBS of light excited in water (see Table 2). The length of active medium was 3 cm (the same as for Ag and Au suspensions). SBS was registered only in the backward direction. SBS maximum conversion efficiency was 10% (less than for Ag and Au suspensions), but the SBS threshold was also less, 0.07 GW/cm^2. Energetical characteristics of SLFRS are close to the parameters of SBS but there are two different features that define possible SLFRS applications: (1) SLFRS propagates in both forward and backward directions with the same frequency shift; and (2) SLFRS frequency shift can easily be varied by choosing the nanoparticle size. Due to these features SLFRS can be used as an effective source of biharmonic pumping with variable frequency shift in gigahertz and terahertz range.

This work was supported by the Russian Foundation for Basic Research (grants 12-03-00396-a and 11-02-01269-a).

References

1. E. Duval, A. Boukenter, and B. Champagnon, Phys. Rev. Lett. **56**, 2052 (1986).
2. H. Lamb, Proc. Lond. Math. Soc. **s1-13**, 189 (1881).
3. E. Duval, Phys. Rev. B **46**, 5795 (1992).
4. A. Tamura, K. Higeta, and T. Ichinokawa, J. Phys. C **15**, 4975 (1982).
5. S. Rufo, M. Dutta, and M. A. Stroscio, J. Appl. Phys. **93**, 2900 (2003).
6. P. Verma, W. Cordts, G. Irmer, and J. Monecke, Phys. Rev. B **60**, 5778 (1999).
7. A. Tanaka, S. Onari, and T. Arai, Phys. Rev. B **47**, 1237 (1993).
8. L. Saviot, B. Champagnon, E. Duval, I. A. Kudriavtsev, and A. I. Ekimov, J. Non-Cryst. Solids **197**, 238 (1996).
9. R. W. Boyd, *Nonlinear Optics* (Academic, 2002).
10. N. V. Tcherniega and A. D. Kudryavtseva, J. Surf. Invest. **3**, 513 (2009).
11. N. V. Tcherniega, M. I. Samoylovich, A. D. Kudryavtseva, A. F. Belyanin, P. V. Pashchenko, and N. N. Dzbanovski, Opt. Lett. **35**, 300 (2010).
12. S. Y. Vasil'eva, A. Y. Olenin, G. I. Romanovskaya, Y. A. Krutyakov, V. I. Pogonin, A. S. Korotkov, and B. K. Zuev, J. Anal. Chem. **64**, 1214 (2009).